**WRINKLE RIDGE-LOBATE SCARP TRANSITION OF WEST SERENITATIS: INDICATIONS FOR RECENT TECTONIC ACTIVITY.** J. D. Clark[1], C. H. van der Bogert[1], H. Hiesinger[1], and H. Bernhardt[1], [1] Institut für Planetologie, Westfälische Wilhelms-Universität, Wilhelm-Klemm-Str. 10, 49149 Münster, Germany (j.clark@uni-muenster.de).

**Introduction:** Lobate scarps and wrinkle ridges are common compressional tectonic landforms on the Moon. However, their appearance and formation are not entirely identical [1-6]. Lunar lobate scarps are typically linear or arcuate in shape and have a crisp appearance with few large superposing craters along the fault trace [2,7-10]. Lobate scarps have asymmetric profiles with relatively steep scarp faces and gently sloping back limbs, representative of the fault dip direction [5]. Scarps are found globally and mainly in the anorthositic highlands [10,11]. Furthermore, the faults that created the lobate scarps typically extend to only the upper kilometer of regolith [12]. In contrast, wrinkle ridges exclusively occur within the maria and are largely interpreted to be the surface manifestation of blind thrust faults, wherein horizontal shortening is accommodated by a fault that does not reach the surface [13-17]. Such faults have been suggested to extend to depths between 100's of meters to several kilometers [13,14,18].

Although ridges and scarps are usually observed independently from one another, a wrinkle ridge and lobate scarp located on the western edge of Mare Serenitatis appear to be associated [19]. The entire length of this E-W trending feature is ~19 km. The wrinkle ridge begins directly west of Dorsum Gast, and its sinuous and boulder-covered ridge cross-cuts the mare basalts until reaching the highlands boundary where it transitions to a lobate scarp morphology.

In this study, we investigate the recency of compressional fault movement along the entire ridge-scarp using crater counting methods to investigate whether the fault represents a single or multiple events, and determine its origin.

**Data and Methods:** NAC (Narrow Angle Camera) image data from the Lunar Reconnaissance Orbiter Camera (LROC) were used for this study and processed using Integrated Software for Imagers and Spectrometers (ISIS) [20,21]. Using ArcGIS, count areas and crater size frequency distribution (CSFD) measurements were generated using CraterTools [22]. The CSFDs were plotted and fit with Craterstats [23], using the techniques described in [24]. Derived absolute model ages (AMAs) are based on the chronology function (CF) and production function (PF) of [25], valid for lunar craters >10 m and <100 km in diameter.

To find the optimal crater count technique, we applied multiple methods to the lobate scarp and wrinkle ridge. First, we applied the method of [9], where AMAs are derived for both the hanging wall and footwall surfaces of the fault. However, the up-hill facing limbs of the lobate scarp have steep slopes resulting in anomalously young ages due to mass wasting. For AMAs derived for the margins of the wrinkle ridge, both surfaces were at equilibrium for all crater diameters less than 300 m. Second, the up-hill facing scarp provided an opportunity to take CSFD measurements directly from the scarp face. Typically, a scarp has a steeply sloping scarp face when the fault offsets a near horizontal surface. Here, the scarp geometry is rotated up-hill, instead making the scarp limbs steeply sloping and the scarp face horizontal, therefore, making the technique of [9] impractical. Although successful, this technique could not be used for the wrinkle ridge as the presumed fault face has a steep slope and is completely covered by boulders. Finally, the Buffered Crater Count (BCC) technique was applied to both the lobate scarp and wrinkle ridge due to the sufficient number of craters (>10 m in diameter) superposing both features. The BCC technique determines ages for linear features independently from the surrounding geologic units [26]. As conventional crater counting includes all craters whose centers are inside the measurement areas, the BCC technique only includes those craters that superpose the linear feature. A buffer is calculated from the diameter from each included crater [27].

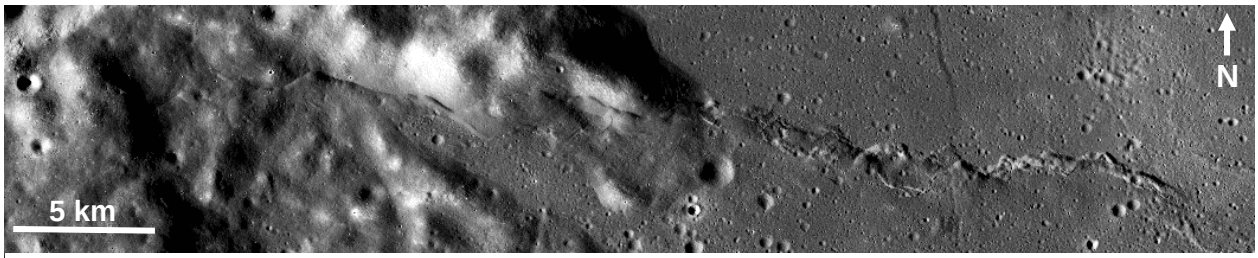


***Figure 1:*** *Kaguya mosaic showing the wrinkle ridge-lobate scarp complex on the western side of Mare Serenitatis. The wrinkle ridge is blanketed by high albedo boulders along the ridge highs and scarp faces. The lobate scarp is up-hill facing with several disconnected segments.*

**Results:** AMAs using the BCC technique (Fig. 2) indicate that the last fault movement for the lobate scarp and wrinkle ridge occurred during the same time at about 50 Ma ago. As the error bars of the AMAs overlap, it is likely that compression occurred concurrently along the entire thrust fault. Moreover, CSFD measurements of the scarp face from all scarp segments show a similar AMA (Fig. 2, green).

Morphological evidence of recent tectonic activity along the wrinkle ridge are the presence of small craters only several 10's of meters wide that contain boulders (Fig. 3) and that the ridge cross-cuts a few craters smaller than ~ 70 m in diameter.

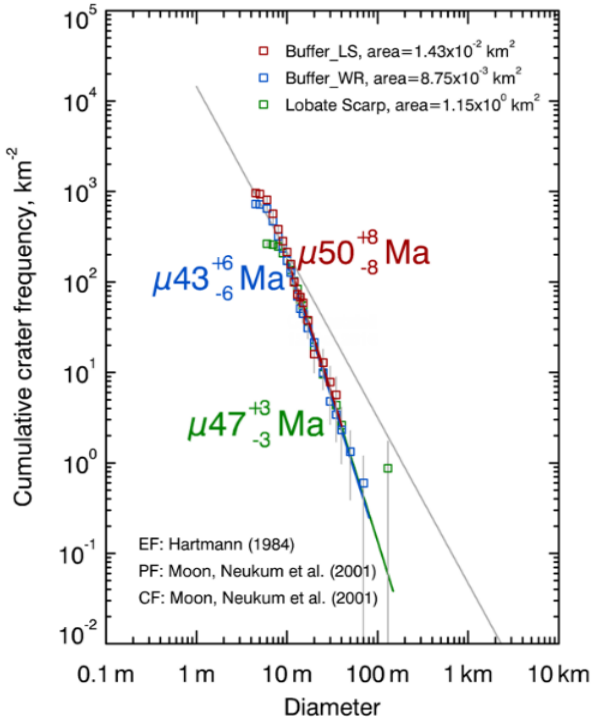


***Figure 2:*** *CSFDs measured for the lobate scarp (LS) and wrinkle ridge (WR). AMAs derived for the lobate scarp (red) and the wrinkle ridge (blue) using the BCC technique overlap within uncertainty. A similar AMA was derived for CSFD measurements of the scarp face from all scarp segments (green).*

**Discussion:** Similar AMAs for the wrinkle ridge and lobate scarp on the western edge of Mare Serenitatis support a link between the two landforms. Wrinkle ridges are postulated to have formed shortly after basalt emplacement in Serenitatis due to basin subsidence [14] (after ~2.44-3.81 Ga [28]). Lobate scarps, however, are one of the youngest landforms on the Moon with derived ages < 700 Ma [8-11]. However, [29] suggested that the presence of high-albedo boulders on the wrinkle ridges indicates seismic shaking from recent tectonic activity. If the formation of the studied wrinkle ridge and lobate scarp structures was simultaneous, either a) the wrinkle ridge is much younger than other ridges in Serenitatis, or b) the pre-existing ridge was reactivated by late-stage compression, extending the thrust fault into the highlands to form the lobate scarp. We propose that the recency of tectonic activity for the ridge-scarp transition west of Serenitatis is likely the result of late-stage global compression typically associated with lobate scarp formation. [30,31] encountered several such ridge-scarp transitions in western Mare Frigoris, and also suggested that the formation of these young tectonic landforms is likely the result of renewed contraction of the lunar surface during late-stage global compressional stress [8,7], while older ridges result from mascon loading.

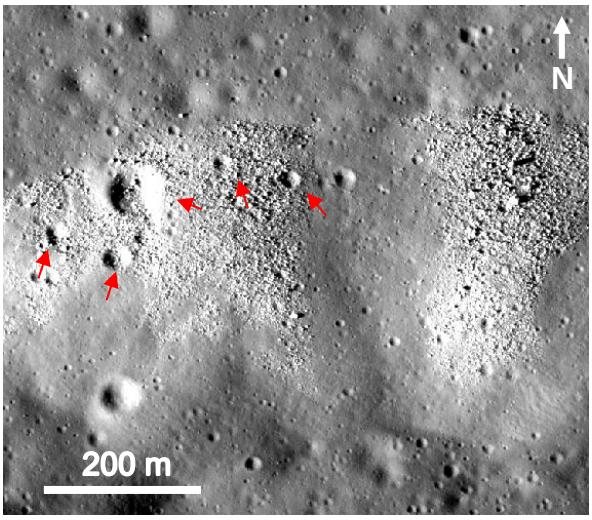


***Figure 3:*** *Boulder outcrops on the wrinkle ridge are characterized by high albedo patches with meters to 10s of meters wide boulders. Small craters on the steep slope are commonly filled by these boulders (red arrows).*

**References:** [1] Watters (2003) *J. Geophys. Res.*, 108. [2] Watters and Schultz (2010) *Planetary Tectonics*, Cambridge Univ. Press. [3] Schultz (1976) *Moon Morphology*, University of Texas Press, Austin, TX. [4] Binder (1982) *Earth, Moon, and Planets*, 26. [5] Watters and Johnson (2010) *Planetary Tectonics*, Cambridge Univ. Press. [6] Watters et al. (2010) *Science*. [7] Binder and Gunga (1985) *Icarus*, 63, 421. [8] van der Bogert et al. (2012) *LPSC XLIII*, Abstract #1847. [9] Clark et al. (2015) *LPSC XLVI*, Abstract #1730. [10] Clark et al. (2016) LPSC XLVII, Abstract #1380. [11] Watters et al. (2015) Geology, 43, 10. [12] Williams et al. (2013) *JGR-Planets*, 118. [13] Schultz (2000) JGR, 205. [14] Solomon and Head (1979) JGR, 84. [15] Solomon and Head (1980) Rev. Geophys. & Space Phys. 18. [16] J.B. Plescia and M.B. Golombek (1986) GSA Bull., 97. [17] Yue et al. (2015) JGR-Planets, 120. [18] Watters (1993), JGR-Planets, 98. [19] Lucchitta (1976) *LPS 7*, 2761-2782. [20] Robinson et al. (2010) Space Sci. Rev. 150, 55. [21] Anderson et al. (2004) *LPSC XXXV*, Abstract #2039. [22] Kneissl et al. (2011) *PSS*, 59. [23] Michael and Neukum (2010) *EPSL*, 294, 223. [24] Neukum (1983) *Meteoritenbombardement und Datierung planetarer Oberflächen*, Habil. Thesis, Univ. Munich. [25] Neukum et al. (2001) Space Sci. Rev., 96, 55. [25] Fassett and Head (2008) *Icarus*, 195. [27] Kneissl et al. (2014) *Icarus*, 250. [28] Hiesinger et al. (2000) JGR, 105, E12. [29] French et al. (2014) *LPSC XLV*, Abstract #2489. [30] Williams et al. (2012) *LPSC XLIII*, Abstract #2708. [31] Williams et al. (2014) *LPSC XLV*, Abstract #2684.